

the δ -sarcoglycan-deficient DCM hamsters. ONO1301-atelocollagen sheet implantation significantly upregulated expression of HGF, VEGF, increased vasculature, attenuated fibrosis, and upregulated α -sarcoglycan in the myocardium and, consequently, preserved cardiac performance and prolonged survival in this hamster DCM model.

Rationale, Feasibility, and Safety of an Atelocollagen Sheet-Based Therapy for IDCM

This study identified cell-dependent and dose-dependent effects of ONO1301 on the release of cardioprotective factors. The cells that were activated by ONO1301 in vitro included skin fibroblasts and CoASMCs. In addition, IPR, which is the sole receptor of ONO1301, was expressed in CoASMCs and endothelial cells, but not in cardiomyocytes or cardiac fibroblasts. These findings suggest that the target cells of ONO1301 may be the vascular SMCs and endothelial cells in the cardiac tissue. Local delivery of ONO1301 into the heart, directly targeting cardiac SMCs and endothelial cells, would thereby theoretically be useful in maximizing the therapeutic effects of ONO1301. In fact, it was shown that the ONO1301-immersed atelocollagen sheet implantation therapy induced marked heart-dominant elevation of the ONO1301 level in association with significantly positive functional effects, indicating rationale and feasibility of this treatment in the IDCM heart. In addition, both the ONO1301 and the atelocollagen sheet only groups did not produce procedure-related mortality despite the deteriorated cardiac function, suggesting the safety of this treatment for IDCM heart.

There are other possible clinically relevant methods for ONO1301 delivery to treat the DCM heart, such as injection of intramyocardial microbeads, systemic intravenous/subcutaneous injection, or oral intake. However, these methods are theoretically limited by possible local damage and/or poor efficiency in the drug delivery to the cardiac tissue⁹ compared with the atelocollagen sheet-based drug delivery system as in this study. Intramyocardial injection of microbeads may also prove to be more efficacious, but further studies will be required to establish the optimal delivery methods of ONO1301 into the heart in preclinical and subsequent clinical studies.

Therapeutic Effects and Underlying Mechanisms of ONO1301 Sheet Therapy

Therapeutic efficiency of this treatment on this δ -sarcoglycan-deficient hamster IDCM model was assured in this

study by comparing with the 2 control groups, in which the sham operation or placement of atelocollagen sheet only was performed. Global systolic cardiac function, assessed by echocardiography, was significantly preserved in the ONO1301-treated hamsters compared with the other groups, and most important, the life expectancy of the J2N-k hamsters was prolonged by this treatment. These important positive findings would be explained by multiple fundamental effects of this treatment, including increased myocardial blood flow, reduction of myocardial fibrosis, and reorganization of cytoskeletal proteins.

It has been reported that ONO1301 acts as an inducer of multiple cardioprotective factors in ischemic cardiac diseases.⁵ Effects of ONO1301 on the IDCM heart, however, are poorly understood. Although the clinical manifestations of end-stage IDCM are similar to those of end-stage ischemic cardiomyopathy, typical IDCM is characterized by a decreased vascular network, increased fibrous components, and decreased expression of cytoskeletal proteins in a global and homogeneous manner.^{10,11} This study also identified multiple endogenous factors upregulated by the ONO1301-atelocollagen sheet, such as HGF, a unique growth factor with antifibrosis and angiogenesis effects,^{8,12} or VEGF, an important mediator of angiogenesis.⁴ In addition, SDF-1 or G-CSF by the ONO1301 treatment in this study may have contributed to therapeutic stem cell homing and activation.^{13,14} Further studies will be required to determine whether these agents induce regenerative responses.

The potential effects of these endogenous factors were well correlated with the pathologic changes in this study, such as increased vasculature, attenuated fibrosis, or upregulated α -sarcoglycan. Of them, increased blood flow may be one of the major mechanisms responsible for the positive therapeutic effects of the ONO1301 in this study. It has been shown that prostacyclin and prostacyclin-inducing HGF/VEGF bring a multiplier effect of vasodilation and new vessel formation responsible to regional ischemic insult.^{15,16} In addition, genetic deletion of IPR had an important role on progression of cardiovascular disease.¹⁵

It is also interesting that cytoskeletal proteins were remodeled by the ONO1301 treatment in this study. Immunohisto-labeling in this study demonstrated the transient reexpression of α -sarcoglycan and α -dystroglycan in the O group. It was speculated that α -sarcoglycan can be recycled from the plasma membrane differently from other sarcoglycans,¹⁷ and inhibition of Smad3 associated with transforming growth factor β signal pathway suppressed by prostacyclin or HGF, brings to α -sarcoglycan gene expression.¹⁸

† $P < .05$ versus ONO1301 (1 nmol/L); # $P < .05$ versus ONO1301 (10 nmol/L); § $P < .05$ versus ONO1301 (100 nmol/L); ‡ $P < .05$ versus ONO1301 (1000 nmol/L). *NHDF*, Normal human dermal fibroblast; *HCoASM/C*, human coronary artery smooth muscle cell; *HGF*, hepatic growth factor; *VEGF*, vascular endothelial growth factor; *SDF-1*, stromal cell-derived factor-1; *PCR*, polymerase chain reaction; *G-CSF*, granulocyte colony stimulating factor; *ELISA*, enzyme-linked immunosorbent assay; *DMSO*, dimethyl sulphoxide; *cAMP*, cyclic aminophosphatase; *n.s.*, not significant.

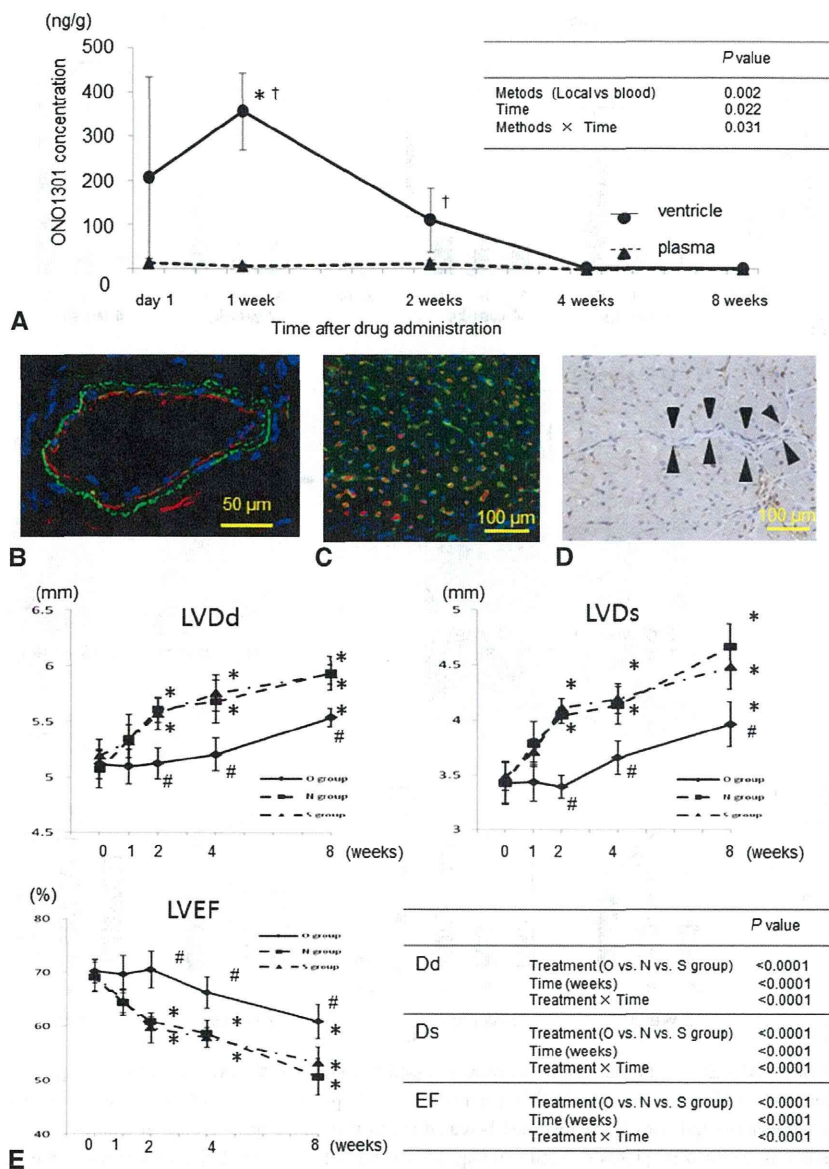


FIGURE 2. Levels of ONO1301 in cardiac tissue and plasma were serially quantified after implantation of ONO1301-eluted atelocollagen sheet for the DCM heart (A). ONO1301 is detected in both samples for 2 weeks after treatment, while the level of ONO1301 in the ventricle is significantly and markedly higher than in the plasma at weeks 1 and 2 after the treatment. * $P < .05$ versus 8 weeks; † $P < .05$ versus plasma concentration. Immunofluorescence staining for IPR and alpha-actin in the DCM heart shows that IPR is positive in the vascular smooth muscle cells and the endothelial cells (B and C). Green, Filamentous-actin; red, IPR; blue, nuclei. 3,3'-diaminobenzidine staining, which produces a brown color, shows that IPR is expressed in the microvasculature, but not in cardiac fibroblasts and cardiomyocytes (arrowhead, cardiac fibroblast) (D). Changes in LVDD/Ds, and LVEF after treatment were serially measured by transthoracic echocardiography (E). These 4 parameters of the LV are preserved until 4 weeks after ONO1301 treatment compared with the other groups. However, ONO1301 treatment does not arrest the progression in dilatation of the dimensions and deterioration of the EF in the subsequent 4 weeks. # $P < .05$ versus N and S group; * $P < .05$ versus 0 weeks. DCM, Dilated cardiomyopathy; LV, left ventricular (ventricle); Dd/Ds, diastolic/systolic dimensions; EF, ejection fraction; IPR, prostacyclin receptor.

Moreover, regarding the transient reexpression of α -dystroglycan, Kondoh and associates⁹ suggested that the reconstruction of α -dystroglycan may occur because the sarcoglycan might mask the matrix metalloproteinase cleavage site on dystroglycan and/or matrix metalloproteinase activity might be inhibited by HGF. In addition, β -sarcoglycan was rarely expressed after the ONO1301 treatment in our

study. Kawada and colleagues¹⁹ reported that both β - and δ -sarcoglycan were completely missing, but α - and γ -sarcoglycan were weakly expressed in the J2N-k hamster, and transfer of the δ -sarcoglycan gene could express not only δ - but the other 3 sarcoglycans. These findings might suggest the limitation of this drug therapy for reorganization of cytoskeletal proteins, but Hack and coworkers²⁰ reported that the

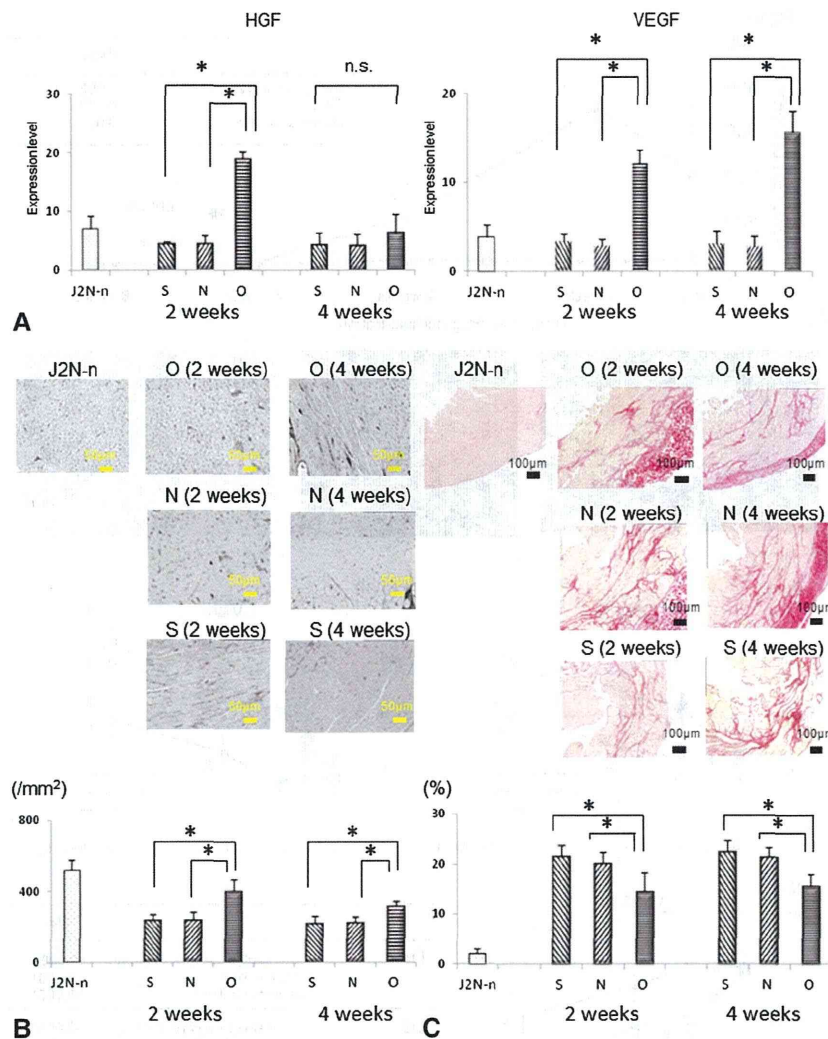


FIGURE 3. Expressions of HGF and VEGF in the cardiac tissue were assessed by real-time PCR, which shows greater expression of the 2 factors in the O group at 2 and 4 weeks compared with the other groups ($n = 5$ for each group) (A). Capillary density in the hearts was assessed by immunohistochemical labeling for vWF, which shows a greater number of capillaries in the ONO1301-treated hearts than in the other groups at 2 and 4 weeks ($n = 5$ for each group) (B). Interstitial fibrosis in the heart was assessed by picrosirius red staining, which shows less accumulation of fibrosis in the ONO1301-treated hearts than in the other groups at 2 and 4 weeks ($n = 5$ for each group) (C). * $P < .05$ versus O group. HGF, Hepatic growth factor; VEGF, vascular endothelial growth factor; PCR, polymerase chain reaction. vWF, von Willebrand factor.

expression of sarcoglycans, even in small amounts, prevented the damage of cardiomyocyte. Reorganization of α -sarcoglycan by the ONO1301 therapy might thus contribute to preserve cardiac function.

Although the level of prostacyclin in the heart in response to the ONO1301 treatment was not investigated in this study, it may be paradoxically elevated by the thromboxane synthase inhibitory activity of the ONO1301 on the heart,²¹ possibly producing synergistic positive effects on the IDCM heart. In addition, it is interesting to research the involvement of the neurohormonal activations in the heart, such as adrenergic system, plasma renin activity, or endothelin, by the ONO1301 treatment.²²

Clinical Perspectives

The atelocollagen sheet-based local ONO1301 delivery therapy globally reversed reduced vascular density, increased fibrosis, and reduced cytoskeletal proteins in the myocardium, all of which were the typical pathologic features in the human IDCM heart,^{10,11} suggesting potential therapeutic benefits of this treatment for IDCM in the clinical scenario. In addition, safety of this treatment shown in this study warrants further preclinical study, including dose-response relation to explore minimum and maximal effective dose of the ONO1301 in the "GLP" standard. A very narrow dose necessary to achieve a positive response may prohibit this agent from clinical trials.

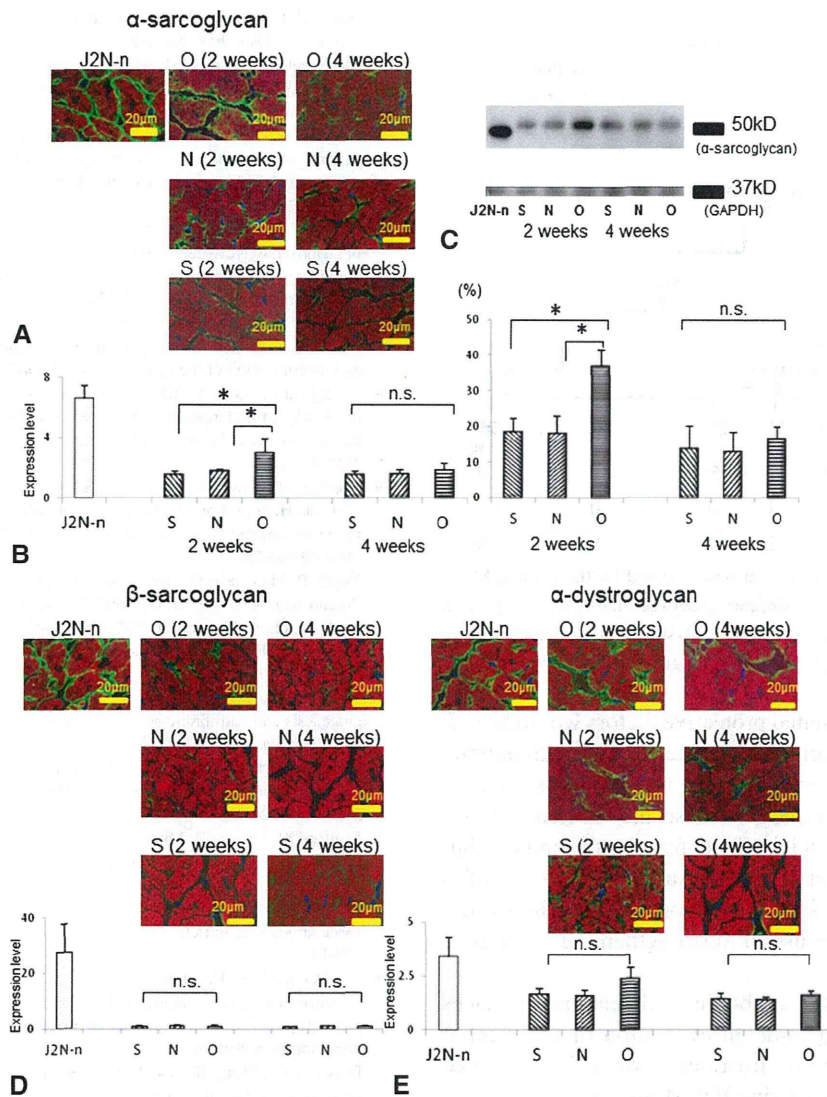


FIGURE 4. Expression of α -sarcoglycan, β -sarcoglycan, and α -dystroglycan in the heart after ONO1301 treatment was assessed by immunohistochemistry, real-time PCR, and Western blot analysis. Immunohistochemistry shows that α -sarcoglycan is clearly expressed around the cardiomyocytes in the normal hamsters, but not in the N or S group (A). Of note, α -sarcoglycan is expressed in the O group at 2 weeks but not at 4 weeks. Green, α -Sarcoglycan; red, filamentous-actin; blue, nuclei. Quantitative real-time PCR shows a significantly greater expression of α -sarcoglycan in the O group than in the N or S group at 2 weeks, but not at 4 weeks ($n = 5$ for each group at each time point, $*P < .05$ vs O group) (B). Consistently, Western blot analysis and the quantitative results of band intensities, which are expressed as a percentage of the value of the J2N-n hamsters, show significantly greater expression of α -sarcoglycan in the O group than in the N or S group at 2 weeks, but not at 4 weeks ($n = 5$ for each group at each time point, $*P < .05$ vs O group) (C). Expression of β -sarcoglycan in the DCM hamsters is not detected even after ONO1301 treatment (D). Green, β -sarcoglycan; red, filamentous-actin; blue, nuclei. α -Dystroglycan is rarely expressed in the N or S group, although its expression is upregulated in the O group (E). There are no significant differences between the O group and the other groups at 2 weeks. Green, α -Dystroglycan; red, filamentous-actin; blue, nuclei. PCR, Polymerase chain reaction; *n.s.*, not significant.

Re-treatment of epicardial implantation of the sheet containing ONO1301 might be technically challenging; however, technical modulation of microsphere generation, such as gelatin hydrogel, might induce further developments to generate a longer-release drug-delivery system than the method used in the present study.²³

Study Limitations

This study was limited by use of a transgenic rodent model. The δ -sarcoglycan-deficient IDCM model used in this study is not completely relevant to human IDCM that shows a number of etiologic and pathologic variations. However, positive functional and pathologic effects

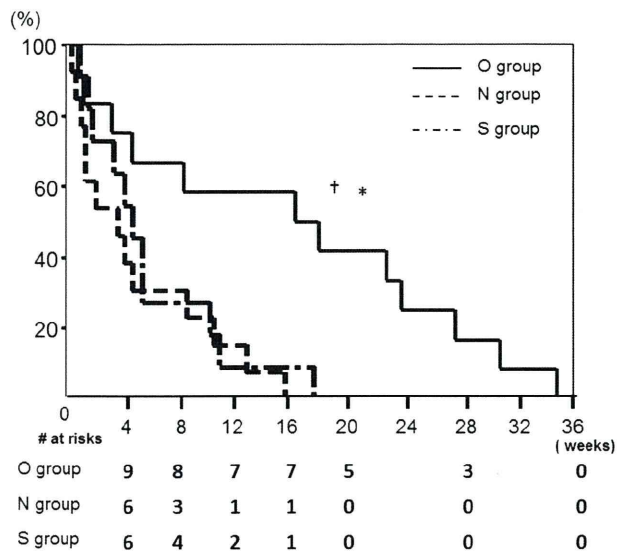


FIGURE 5. Survival after treatment was assessed by the Kaplan-Meier method. There is no significant difference between the N (n = 11) and S groups (n = 13), whereas the O group (n = 12) shows a significantly greater survival than the other groups (* $P < .05$ vs S group; † $P < .05$ vs N group).

associated with upregulated protective factors would be sufficient to prove the principal concept of this treatment. Agents that are beneficial in these mutant hamsters may not be beneficial in humans because the mechanisms responsible for the beneficial effects may be different in humans. However, further pathologic and functional studies for human DCM heart samples, in comparison with the deficient hamster, may be useful to strengthen the findings of this study.

Poor availability of the antibodies and genome sequences in the hamster limited in-depth evaluation of the mechanisms responsible for this treatment, which is warranted to be supplemented by murine IDCM model.²⁴

CONCLUSIONS

ONO1301 reorganized cytoskeletal proteins, especially α -sarcoglycan, increased capillaries, and reduced fibrosis through the upregulation of cardiac protective factors, leading to functional recovery and prolonged survival in the δ -sarcoglycan-deficient IDCM hamster. A preclinical study to explore the optimal, clinically relevant protocol is warranted.

We thank Masako Yokoyama, Akima Harada, and Motoko Shiozaki for their excellent technical assistance.

References

- Rajnoch C, Chachques JC, Berrebi A, Bruneval P, Benoit MO, Carpentier A. Cellular therapy reverses myocardial dysfunction. *J Thorac Cardiovasc Surg.* 2001; 121:871-8.
- Nakamura T, Matsumoto K, Mizuno S, Sawa Y, Matsuda H, Nakamura T. Hepatocyte growth factor prevents tissue fibrosis, remodeling, and dysfunction in cardiomyopathic hamster hearts. *Am J Physiol Heart Circ Physiol.* 2005;288:H2131-9.
- Juan CC. Cellular cardiac regenerative therapy in which patients? *Expert Rev Cardiovasc Ther.* 2009;7:911-9.
- Matsumoto K, Okazaki H, Nakamura T. Novel function of prostaglandins as inducers of gene expression of HGF and putative mediator of tissue regeneration. *J Biochem.* 1995;117:458-64.
- Iwata H, Nakamura K, Sumi M, Ninomiya M, Sakai Y, Sata M, et al. Local delivery of synthetic prostacyclin agonist augments collateral growth and improves cardiac function in a swine chronic cardiac ischemia model. *Life Sci.* 2009;85:255-61.
- Mitsuhashi S, Saito N, Watano K, Igarashi K, Tagami S, Kikuchi K, et al. Defect of Delta-sarcoglycan gene is responsible for development of dilated cardiomyopathy of a novel hamster strain, J2N-k: calcineurin/PP2B activity in the heart of J2N-k hamster. *J Biochem.* 2003;134:269-76.
- Saini SG, Wani AT, Vashney B, Ahmed T, Rajan SK, Paliwal LJ. Validation of the LC-MS/MS method for the quantification of mevalonic acid in human plasma and determination of the matrix effect. *J Lipid Res.* 2006;47:2340-5.
- Miyagawa S, Sawa Y, Taketani S, Kawaguchi N, Nakamura T, Matsuda H, et al. Myocardial regeneration therapy for heart failure: hepatocyte growth factor enhances the effect of cellular cardiomyoplasty. *Circulation.* 2002; 105:2556-61.
- Kondoh H, Sawa Y, Miyagawa S, Matsumiya S, Sakakida-Kitagawa S, Matsuda H, et al. Longer preservation of cardiac performance by sheet-shaped myoblast implantation in dilated cardiomyopathic hamsters. *Cardiovasc Res.* 2006;69:466-75.
- Neglia D, Michelassi C, Trivieri MG, Sambucetti G, Giorgetti A, Parodi O, et al. Prognostic role of myocardial blood flow impairment in idiopathic left ventricular dysfunction. *Circulation.* 2002;105:186-93.
- Towbin JA. The role of cytoskeletal proteins in cardiomyopathies. *Curr Opin Cell Biol.* 1998;10:131-9.
- Taniyama Y, Morishita R, Aoki M, Hirooka K, Yamasaki K, Ogihara T, et al. Angiogenesis and antifibrotic action by hepatocyte growth factor in cardiomyopathy. *Hypertension.* 2002;40:47-53.
- Saxena A, Fish JE, White MD, Yu S, Smyth JW, Srivastava D, et al. Stromal cell-derived factor-1 α is cardioprotective after myocardial infarction. *Circulation.* 2008;117:2224-31.
- Stanford SJ, Pepper JR, Mitchell JA. Release of GM-CSF and G-CSF by human arterial and venous smooth muscle cell: differential regulation by COX-2. *Br J Pharmacol.* 2000;129:835-8.
- Fetalvero KM, Martin KA, Hwa J. Cardioprotective prostacyclin signaling in vascular smooth muscle cell. *Prostaglandins Other Lipid Mediat.* 2007;82: 109-18.
- Hiraoka K, Koike H, Yamamoto S, Tomita N, Yokoyama C, Morishita R, et al. Enhanced therapeutic angiogenesis by cotransfection of prostacyclin synthase gene or optimization of intramuscular injection of naked plasmid DNA. *Circulation.* 2003;108:2689-96.
- Draviam RA, Wang B, Shand SH, Xiao X, Watkins SC. Alpha-sarcoglycan is recycled from the plasma membrane in the absence of sarcoglycan complex assembly. *Traffic.* 2006;7:793-810.
- Hernández-Hernández JM, Delgado-Olguín P, Aguillón-Huerta V, Furlan-Magaril M, Recillas-Targa F, Coral-Vázquez RM. Sox9 represses alpha-sarcoglycan gene expression in early myogenic differentiation. *J Mol Biol.* 2009;394:1-14.
- Kawada T, Nakaturu Y, Sakamoto A, Koizumi T, Shin WS, Toyooka T, et al. Strain- and age-dependent loss of sarcoglycan complex in cardiomyopathic hamster hearts and its re-expression by delta-sarcoglycan gene transfer in vivo. *FEBS Lett.* 1999;458:405-8.
- Hack AA, Lam MY, Cordier L, Shoturma DI, Ly CT, Hadhazy MA. Differential requirement for individual sarcoglycans and dystrophin in the assembly and function of the dystrophin-glycoprotein complex. *J Cell Sci.* 2000; 113:2535-44.
- Yamanaka S, Miura K, Yukimura T, Okumura M, Yamamoto K. Putative mechanism of hypotensive action of platelet-activating factor in dogs. *Circ Res.* 1992; 70:893-901.
- Somova LI, Mufunda JJ. Renin-angiotensin-aldosterone system and thromboxane A2/prostacyclin in normotensive and thromboxane A2/prostacyclin in normotensive and hypertensive black Zimbabwans. *Ethn Dis.* 1992;2:27-34.
- Takaoka R, Hikasa Y, Hayashi K, Tabata Y. Bone regeneration by lactoferrin released from a gelatin hydrogel. *J Biomater Sci Polym Ed.* 2010;22:1581-9.
- Lu D, Ma Y, Zhang W, Bao D, Dong W, Zhang L, et al. Knockdown of cytochrome P450 2E1 inhibits oxidative stress and apoptosis in the cTnT (R141W) dilated cardiomyopathy transgenic mice. *Hypertension.* 2012;60:81-9.

Impact of cardiac support device combined with slow-release prostacyclin agonist in a canine ischemic cardiomyopathy model

Yasuhiko Kubota, MD,^a Shigeru Miyagawa, MD, PhD,^a Satsuki Fukushima, MD, PhD,^a Atsuhiko Saito, PhD,^a Hiroshi Watabe, PhD,^b Takashi Daimon, PhD,^c Yoshiki Sakai, PhD,^a Toshiaki Akita, MD, PhD,^d and Yoshiki Sawa, MD, PhD^a

Background: The cardiac support device supports the heart and mechanically reduces left ventricular (LV) diastolic wall stress. Although it has been shown to halt LV remodeling in dilated cardiomyopathy, its therapeutic efficacy is limited by its lack of biological effects. In contrast, the slow-release synthetic prostacyclin agonist ONO-1301 enhances reversal of LV remodeling through biological mechanisms such as angiogenesis and attenuation of fibrosis. We therefore hypothesized that ONO-1301 plus a cardiac support device might be beneficial for the treatment of ischemic cardiomyopathy.

Methods: Twenty-four dogs with induced anterior wall infarction were assigned randomly to 1 of 4 groups at 1 week postinfarction as follows: cardiac support device alone, cardiac support device plus ONO-1301 (hybrid therapy), ONO-1301 alone, or sham control.

Results: At 8 weeks post-infarction, LV wall stress was reduced significantly in the hybrid therapy group compared with the other groups. Myocardial blood flow, measured by positron emission tomography, and vascular density were significantly higher in the hybrid therapy group compared with the cardiac support device alone and sham groups. The hybrid therapy group also showed the least interstitial fibrosis, the greatest recovery of LV systolic and diastolic functions, assessed by multidetector computed tomography and cardiac catheterization, and the lowest plasma N-terminal pro-B-type natriuretic peptide levels ($P < .05$).

Conclusions: The combination of a cardiac support device and the prostacyclin agonist ONO-1301 elicited a greater reversal of LV remodeling than either treatment alone, suggesting the potential of this hybrid therapy for the clinical treatment of ischemia-induced heart failure. (J Thorac Cardiovasc Surg 2014;147:1081-7)

Left ventricular (LV) remodeling in ischemic and nonischemic dilated cardiomyopathy is characterized by progressive dilatation and dysfunction of the left ventricle, leading to severe heart failure.^{1,2} The cardiac support device is a mesh net designed to reduce diastolic ventricular wall stress by mechanical means and thus prevent LV dilatation. It has been shown to halt LV remodeling in dilated cardiomyopathy in preclinical studies.³⁻⁵ Clinical trials undertaken on the basis of these favorable results showed beneficial effects on LV remodeling, including significantly decreased LV end-systolic (LVESV) and end-diastolic volumes (LVEDV), and a significant improvement in New York Heart Association functional class.⁶⁻⁸

However, despite these positive effects, the device has not been associated with reductions in mortality and has not been approved for clinical use.⁹

The synthetic prostacyclin agonist ONO-1301 acts as a myocardial regenerative biological drug to enhance reversal of LV remodeling.¹⁰⁻¹² The beneficial effects of ONO-1301 on the heart are mediated by up-regulation of angiogenic and antifibrotic molecules, such as hepatocyte growth factor (HGF), vascular endothelial growth factor (VEGF), and stromal cell-derived factor-1 (SDF-1).¹⁰⁻¹² This mechanism has been shown to result in the active suppression of ischemic and fibrotic changes in the myocardium.¹⁰⁻¹²

We hypothesized that the biological effects of the slow-release form of the synthetic prostacyclin agonist ONO-1301 might complement the mechanical effects of the cardiac support device, thus enhancing its therapeutic effects in ischemic cardiomyopathy.

MATERIALS AND METHODS

All animals used in this study received care in compliance with the Guide for the Care and Use of Laboratory Animals (National Institutes of Health publication no. 85-23, revised 1996).

Animal Treatment

A total of 28 beagles (Oriental Yeast, Co, Ltd, Tokyo, Japan) weighing 9 to 11 kg were used. General anesthesia was administered with intramuscular ketamine (10 mg/kg) and intravenous propofol (5 mg/kg) for induction,

From the Department of Cardiovascular Surgery,^a Department of Molecular Imaging in Medicine,^b Osaka University Graduate School of Medicine, Osaka, Japan; Department of Biostatistics,^c Hyogo College of Medicine, Hyogo, Japan; Department of Cardiovascular Surgery,^d Kanazawa Medical University, Ishikawa, Japan.

Supported by the New Energy and Industrial Technology Organization and the Japan Society for the Promotion of Science Core-to-Core Program.

Disclosures: Authors have nothing to disclose with regard to commercial support. Received for publication Feb 12, 2013; revisions received May 9, 2013; accepted for publication May 16, 2013; available ahead of print Oct 15, 2013.

Address for reprints: Yoshiki Sawa, MD, PhD, Department of Cardiovascular Surgery, Osaka University Graduate School of Medicine, 565-0871, 2-2 Yamadaoka, Suita, Osaka, Japan (E-mail: sawa-p@surg1.med.osaka-u.ac.jp).

0022-5223/\$36.00

Copyright © 2014 by The American Association for Thoracic Surgery

<http://dx.doi.org/10.1016/j.jtcvs.2013.05.035>

Abbreviations and Acronyms

ANOVA	= analysis of variance
dp/dt	= delta pressure/delta time
Ees	= end-systolic elastance
HGF	= hepatocyte growth factor
LV	= left ventricular
LVEDV	= left ventricular end-diastolic volume
LVESV	= left ventricular end-systolic volume
MDCT	= multidetector computed tomography
MI	= myocardial infarction
NT-proBNP	= amino-terminal pro-brain natriuretic peptide
SDF-1	= stromal cell-derived factor-1
VEGF	= vascular endothelial growth factor

and inhaled sevoflurane (1%–2%) for subsequent maintenance, with endotracheal intubation and mechanical ventilator support. After completion of the experiments, the animals were killed under general anesthesia, using an overdose of intravenous sodium pentobarbital (18 mg/kg) to achieve complete sedation, followed by administration of an intravenous potassium-based solution.

Myocardial Infarction Induction

With the animals under general anesthesia, a minimal left thoracotomy was performed through the fifth intercostal space, and the heart was exposed by pericardiotomy. The left descending artery and diagonal vessels were ligated both proximally and distally using 5-0 polypropylene sutures to produce an anterior myocardial infarction (MI). Akinesis of the anterior wall was confirmed by epicardial echocardiography and the chest was closed in layers. The animals were allowed to recover.

Cardiac Support Device

The cardiac support device (0.9–1.0 g), made from polyglycolic acid (Nipro Corporation, Osaka, Japan), was designed on the basis of data obtained from multidetector computed tomography (MDCT) and a heart excised at 1 week postinfarction.

Treatments

The animals were assigned randomly to 1 of 4 groups at 1 week after infarct induction as follows: cardiac support device alone, cardiac support device plus ONO-1301 (hybrid therapy), ONO-1301 alone, or sham control group. In the cardiac support device alone group, 2 sheets of atelocollagen (50 × 50 mm) (Integran; Nippon Zoki Pharmaceutical Co, Ltd, Osaka, Japan) immersed in suspended polylactic and glycolic acid (10 mg/kg) were fixed on the whole surface of the ventricles and the cardiac support device was placed as described previously.³⁻⁵ The same procedure was used in the hybrid therapy group, with the addition of ONO-1301¹⁰⁻¹² (10 mg/kg) (ONO Pharmaceutical Co, Ltd, Osaka, Japan) instead of the polylactic and glycolic acid. In the ONO-1301 alone group, 2 sheets of atelocollagen (50 × 50 mm) immersed in suspended ONO-1301 (10 mg/kg) were fixed on the whole surface of the ventricles. The sham group was subjected to the same procedures as the ONO-1301 alone group, except for the use of polylactic and glycolic acid instead of ONO-1301.

Transthoracic Echocardiography

Transthoracic echocardiography was performed using a 5.0-MHz transducer (Altida; Toshiba Medical Systems Corporation, Tochigi, Japan)

for 2-dimensional speckle-tracking echocardiography under general anesthesia. The data were analyzed using 2-dimensional Wall Motion Tracking software (Toshiba Medical Systems Corporation) as previously described.¹³

MDCT

Electrocardiography-gated MDCT was performed using a 16-row MDCT scanner (SOMATOM Emotion 16-Slice Configuration; Siemens, Munich, Germany) during an end-expiratory breath-hold under general anesthesia. MDCT was performed after intravenous injection of 30 mL of nonionic contrast medium (Iomeron; Bracco, Milan, Italy). All images were analyzed on a workstation (AZE VirtualPlace Lexus64; AZE, Tokyo, Japan). LVEDV and LVESV, LV ejection fraction, LV end-diastolic and end-systolic sphericity indices, and LV/right ventricular end-diastolic and end-systolic diameter values were obtained from the workstation.

Cardiac Catheterization

Under general anesthesia, a 3F micromanometer-tipped catheter (SPR-249; Millar Instruments, Houston, Tex) was inserted through the ventricular apex via a left thoracotomy to measure hemodynamic parameters and cardiac functions, including end-systolic pressure and end-diastolic pressure, delta pressure/delta time (dp/dt) maximum, dp/dt minimum, end-systolic elastance (Ees), and the time constant of relaxation in the left and right ventricles. LV volume was altered by occluding the inferior vena cava with tape via a left thoracotomy.

Wall Stress Calculation

LV wall stress was evaluated using specifically developed software (YD, Ltd, Tokyo, Japan) on an off-line personal computer. Global end-systolic and end-diastolic wall stresses were calculated on the basis of the data obtained from MDCT and cardiac catheterization.¹⁴

Cardiac Positron Emission Tomography

¹³N-ammonia (200–300 MBq) positron emission tomography (PET) was performed using a HeadtomeV/SET2400W (Shimadzu, Co, Kyoto, Japan) under general anesthesia. Myocardial blood flow was quantitated using PMOD software (version 3.2) (PMOD Technologies, Ltd, Zurich, Switzerland) and divided into 17 segments as recommended by the American Heart Association.

Histologic Analysis

Paraffin-embedded transverse sections of the excised hearts were stained with periodic acid-Schiff to measure the short-axis diameter of the myocytes, and with Masson trichrome to assess the extent of fibrosis. The sections were immunostained with anti-CD31 antibody in LSAB kits (DakoCytomation, Glostrup, Denmark). Myocyte diameters and vascular density were measured in 10 different randomly selected fields using a Biorevo BZ-9000 fluorescence microscope (Keyence, Osaka, Japan), and percentage fibrosis was calculated using MetaMorph software (Molecular Devices, Tokyo, Japan).

Real-Time Polymerase Chain Reaction

Total RNA extracted from cardiac tissue was reverse-transcribed using TaqMan reverse transcription reagents (Applied Biosystems, Foster City, Calif), and assayed using the ABI PRISM 7700 (Applied Biosystems). The average copy number of gene transcripts was normalized to that of glyceraldehyde 3-phosphate dehydrogenase for each sample.

Statistical Analysis

All statistical analyses were performed using JMP software (JMP9; SAS institute, Inc, Cary, NC). Results are presented as the mean ± standard deviation. Cardiac catheterization and histologic data were compared by 1-way analysis of variance (ANOVA). MDCT, echocardiography, wall stress, and amino-terminal pro-brain natriuretic peptide (NT-proBNP)

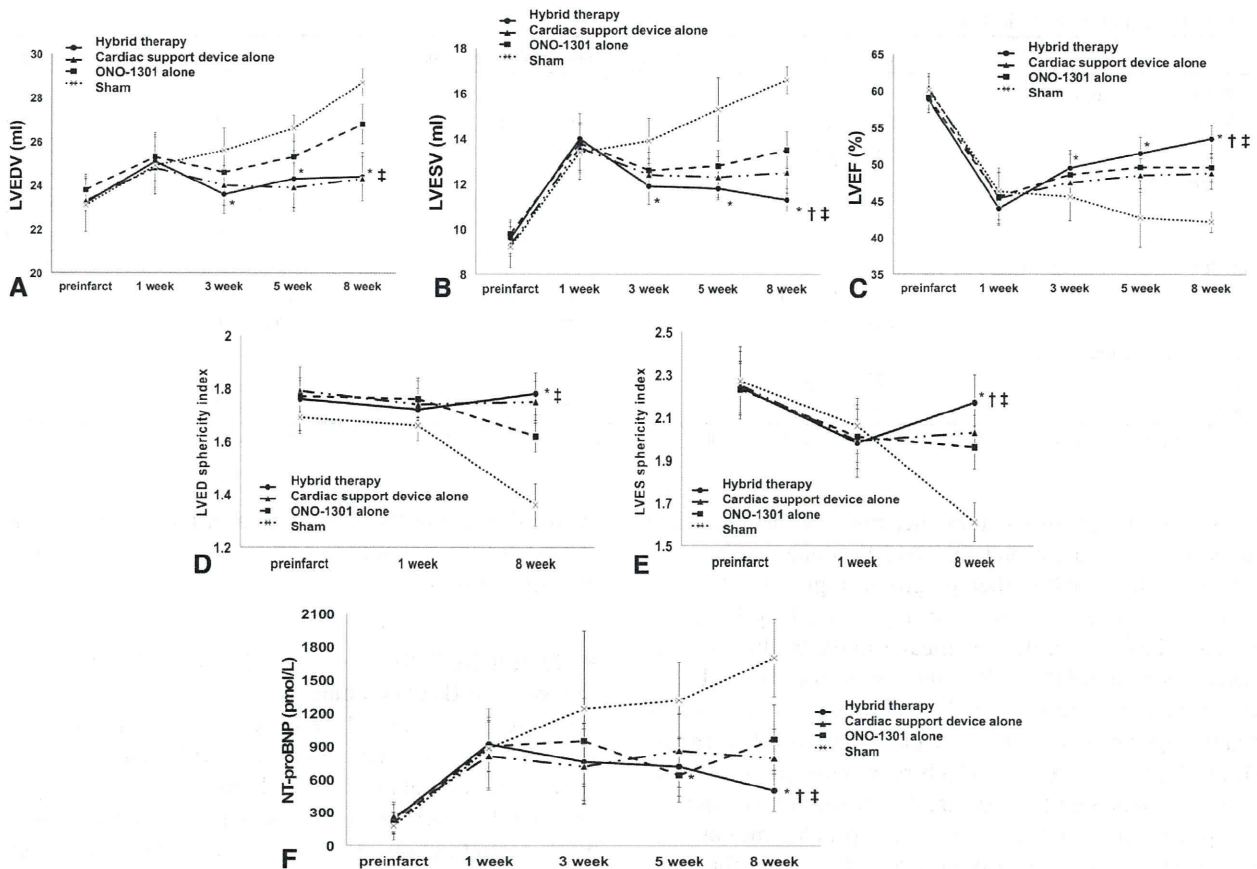


FIGURE 1. MDCT analysis. A, Changes in LVEDV. B, Changes in LVESV. C, Changes in LV ejection fraction. D, Changes in left ventricular end-diastolic and, (E) end-systolic sphericity indices. F, Changes in NT-proBNP. Hybrid therapy is shown by circles with a solid line, a cardiac support device alone is shown by triangles with a dashed/dotted line, ONO-1301 alone is shown by squares with a dashed line, and sham is shown by crosses with a dotted line. * $P < .05$ versus corresponding sham, † $P < .05$ versus corresponding cardiac support device alone, ‡ $P < .05$ versus corresponding ONO-1301 alone. LV sphericity index, LV long-axis diameter/LV short-axis diameter. LVEDV, Left ventricular end-diastolic volume; LVESV, left ventricular end-systolic volume; NT-proBNP, amino-terminal pro-brain natriuretic peptide.

data were compared by repeated ANOVA, using values obtained by subtracting the values at 1 week postinfarction from the values at each time point. Significant differences shown by ANOVA were subjected to post hoc analysis with Bonferroni correction. Sample size justification was not performed. A P value less than .05 was considered statistically significant.

RESULTS

Procedure-Related Morbidity and Mortality

Twenty-four animals completed the study. Three of the animals that failed to complete the study died within 1 week postinfarction and the remaining animal, which was a sham control, died at 7 weeks postinfarction. No dogs developed infections or had insufficient MI.

Recovery of Global Cardiac Performance With Hybrid Therapy

Global cardiac performance after the treatment was assessed serially and comprehensively by MDCT and cardiac

catheterization. Both LVEDV and LVESV tended to increase after MI induction in the sham group (Figure 1, A and B). LVEDV was significantly smaller in the hybrid therapy group compared with the sham group at 3 and 5 weeks postinfarction, and significantly smaller than in both the ONO-1301 alone and sham groups at 8 weeks postinfarction. LVESV in the hybrid therapy group was significantly smaller than that in the sham group at 3 and 5 weeks, and was significantly smaller than that in the other groups at 8 weeks. As a result, LV ejection fraction was significantly greater in the hybrid therapy group compared with the sham group at 3 and 5 weeks, and significantly greater than in the other groups at 8 weeks (Figure 1, C).

The LV end-diastolic sphericity index was significantly greater in the hybrid therapy group compared with the ONO-1301 alone and sham groups at 8 weeks postinfarction (Figure 1, D). The LV end-systolic sphericity index decreased in all groups at 1 week postinfarction, whereas at 8 weeks the LV end-systolic sphericity index had decreased

ET/BS

TABLE 1. Cardiac catheterization data

	Hybrid therapy	Cardiac support device alone	ONO-1301 alone	Sham
dp/dt maximum (mm Hg/s)				
LV	1822 ± 83*,†,‡	1584 ± 114	1601 ± 91	1238 ± 127
RV	547 ± 101	450 ± 53	539 ± 79	443 ± 86
Ees (mm Hg/mL)				
LV	10 ± 1*,†,‡	7 ± 1	8 ± 1	4 ± 1
RV	3 ± 1	3 ± 1	3 ± 1	2 ± 1
-dp/dt minimum (mm Hg/s)				
LV	1553 ± 61*,†,‡	1303 ± 71	1387 ± 64	1061 ± 107
RV	407 ± 59	378 ± 67	412 ± 88	333 ± 78
Time constant of relaxation (s)				
LV	33 ± 4*,†	42 ± 3	36 ± 3	47 ± 5
RV	39 ± 6	40 ± 2	38 ± 4	46 ± 6

Data are mean ± standard deviation. RV, Right ventricular; LV, left ventricular. * $P < .05$ versus sham. † $P < .05$ versus cardiac support device alone. ‡ $P < .05$ versus ONO-1301 alone.

further in the sham group, remained the same in the cardiac support device alone and ONO-1301 alone groups, and recovered in the hybrid therapy group (Figure 1, E).

In addition, systolic function represented by LV dp/dt max and Ees at 8 weeks was greater in the cardiac support device alone and ONO-1301 alone groups compared with the sham group, whereas the hybrid therapy showed significantly greater dp/dt max and Ees than the other groups (Table 1). LV -dp/dt min, which represents diastolic function, also was significantly greater in the hybrid therapy group at 8 weeks than in the other groups. LV time constant of relaxation, which is also an index of diastolic function, was significantly smaller in the hybrid therapy group at 8 weeks postinfarction than in the cardiac support device alone and sham groups. There were no significant differences in any of these parameters in the right ventricle.

MI induction also resulted in an increase in plasma NT-proBNP, assessed by an enzyme-linked immunosorbent assay kit (Cardiopet proBNP; IDEXX Laboratories, Tokyo, Japan), at 1 week postinfarction (Figure 1, F). NT-proBNP continued to increase in the sham group, whereas the increase was suppressed in each of the other groups after treatment. NT-proBNP decreased gradually in the hybrid therapy group and was significantly lower than in the sham group at 5 weeks, and was significantly lower than in the other 2 groups at 8 weeks.

Functional Recovery of Infarct Border Area With Hybrid Therapy

Regional LV wall motion was evaluated using speckle-tracking echocardiography to dissect region-specific functional effects of the treatment. The infarct area showed a significant and marked reduction in the radial strain after induction of MI, with no significant differences among the 4 groups (Table 2). Radial strain levels in the border area decreased similarly in all groups at 1 week postinfarction, although at 8 weeks the hybrid therapy group showed the greatest recovery in this area. There was a marked decrease

in radial strain in the remote area in the sham group at 8 weeks, but there was little change throughout the study in the other groups.

Reduction in Global End-Systolic/Diastolic Wall Stress With Hybrid Therapy

Changes in global end-systolic/end-diastolic wall stresses after treatment were assessed from MDCT and catheterization data (Table 2). Similar increases in global end-systolic wall stress were observed in all groups at 1 week postinfarction. At 8 weeks postinfarction, however, there was a further increase in the sham group, a slight reduction in the cardiac support device alone group, and almost no change in the ONO-1301 alone group, whereas global end-systolic wall stress was lowest in the hybrid therapy group. Similar increases in global end-diastolic wall stress were observed in all groups at 1 week postinfarction. The sham group showed a marked increase at 8 weeks postinfarction, whereas the hybrid therapy and cardiac support device alone groups showed notable reductions. Global end-diastolic wall stress was significantly lower in the hybrid therapy group compared with the ONO-1301 alone and sham groups at 8 weeks.

ONO-1301 Induced Angiogenic Myocardial Effects in Chronic MI

The angiogenic effects of the treatment were evaluated by assessing global myocardial blood flow at rest by ^{13}N -ammonia PET at 8 weeks postinfarction. Myocardial blood flow in the hybrid therapy group was similar to that in the ONO-1301 group, and both were significantly higher than in the cardiac support device alone and sham groups (Figure 2). Capillary densities in the border and remote areas at 8 weeks postinfarction, which was measured by immunostaining for CD31, was significantly greater in the hybrid therapy group than in the cardiac support device alone and sham groups (Figure 3, A).

TABLE 2. Regional left ventricular wall motion and global left ventricular wall stress

	Hybrid therapy	Cardiac support device alone	ONO-1301 alone	Sham
Radial strain in the MI area (%)				
Pre-infarction	21.4 ± 2.3	20.9 ± 1.0	21.7 ± 2.4	22.4 ± 2.3
1 week post-infarction	7.1 ± 1.0	6.7 ± 0.7	7.5 ± 0.9	7.0 ± 1.0
8 weeks postinfarction	8.7 ± 1.2	7.3 ± 0.4	7.5 ± 1.3	6.7 ± 1.0
Radial strain in the border area (%)				
Pre-infarction	22.2 ± 2.6	21.8 ± 2.5	22.0 ± 1.6	21.3 ± 1.8
1 week postinfarction	10.4 ± 1.9	10.3 ± 1.9	11.2 ± 1.5	11.5 ± 1.9
8 weeks postinfarction	14.7 ± 1.1*,†,‡	10.8 ± 0.2	13.1 ± 1.7	8.1 ± 1.1
Radial strain in the remote area (%)				
Pre-infarction	20.7 ± 2.3	21.6 ± 2.0	21.0 ± 2.8	21.2 ± 2.7
1 week postinfarction	19.2 ± 2.1	20.5 ± 1.2	20.9 ± 2.2	19.6 ± 2.0
8 weeks postinfarction	20.2 ± 1.8*	19.7 ± 1.1	20.1 ± 1.5	14.8 ± 1.4
Global end-systolic wall stress (kdyne/cm ²)				
Pre-infarction	79.9 ± 6.8	84 ± 12.0	80.5 ± 8.1	87.6 ± 9.5
1 week postinfarction	108.1 ± 9.1	104.8 ± 11.9	102.7 ± 11.4	107.5 ± 9.6
8 weeks postinfarction	84 ± 5.7*,†,‡	97.7 ± 11.4	104.6 ± 10.0	161.9 ± 9.3
Global end-systolic wall stress (kdyne/cm ²)				
Pre-infarction	13.0 ± 1.5	11.5 ± 1.1	12.0 ± 1.3	12.0 ± 1.6
1 week postinfarction	17.9 ± 1.5	17.1 ± 1.0	17.0 ± 1.4	16.4 ± 2.5
8 weeks postinfarction	14.0 ± 2.5*,‡	14.0 ± 1.8	18.0 ± 1.5	24.4 ± 3.6

Data are mean ± standard deviation. MI, Myocardial infarction. *P < .05 versus sham. †P < .05 versus cardiac support device alone. ‡P < .05 versus ONO-1301 alone.

Histologic Evidence of Reversal of LV Remodeling With Hybrid Therapy

Pathologic cardiomyocyte hypertrophy and interstitial fibrosis in the border and remote areas at 8 weeks postinfarction were assessed by periodic acid-Schiff and Masson trichrome staining, respectively, to evaluate the degree of reversal of LV remodeling induced by each treatment (Figure 3, B and C). Cardiomyocyte diameters were

significantly smaller in the border area in the hybrid therapy group compared with the ONO-1301 alone and sham groups, and were significantly smaller in the remote area compared with the sham group. In addition, there was significantly less interstitial fibrosis in the hybrid therapy group compared with the cardiac support device alone, ONO-1301 alone, and sham groups in the border area, and less than in the sham group in the remote area.

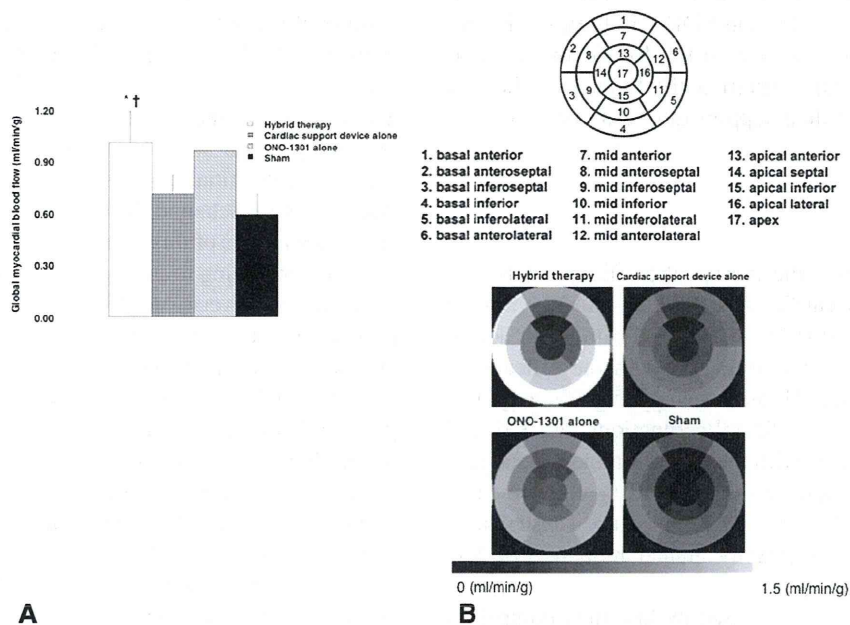


FIGURE 2. A, Global myocardial blood flow assessed by PET at 8 weeks postinfarction. B, Myocardial blood flow divided into 17 segments recommended by the American Heart Association. *P < .05 versus sham, †P < .05 versus cardiac support device alone.